

Facile synthesis, structural and luminescence studies of $\text{MgTiO}_3:\text{Sm}^{3+}$ nanophosphor for display applications

B.M. Thammanna^{1,2}, Dr. V. Senthil Kumar^{2*}

¹ Department of Physics, PES College of Engineering, Mandya-571401, Karnataka, India

² Department of Physics, Karpagam Academy of Higher Education, Eachanari, Coimbatore – 641021, Tamil Nadu, India

*Corresponding author E-mail: senthilkumar.v@kahedu.edu.in.

Abstract

Luminescence properties of combustion prepared $\text{Mg}_2\text{TiO}_3:\text{Sm}^{3+}$ (1-11 mol %) phosphors were studied in the present work. The crystal size (D) was in the range 20- 40 nm as estimated and it was similar to Transmission electron microscopy (TEM) results. The band gap of the materials was in the range 4.45 to 4.87 eV as calculated using Kubelka-Monk function. The PL peaks of Sm^{3+} ions are due to the intra 4-f orbital transitions ($^4\text{G}_{5/2} \rightarrow ^6\text{H}_{5/2}$, $^4\text{G}_{5/2} \rightarrow ^6\text{H}_{7/2}$, $^4\text{G}_{5/2} \rightarrow ^6\text{H}_{9/2}$ and $^4\text{G}_{5/2} \rightarrow ^6\text{H}_{11/2}$). Among the samples, 5 mol % doped one shows the highest PL intensity under 413 nm excitation. The CIE chromaticity coordinates showed orange of red emission (CCT ~2036 K), as a result $\text{Mg}_2\text{TiO}_3:\text{Sm}^{3+}$ (1-11 mol %) Nanophosphors were obviously for solid-state lighting and warm white light emissive display applications.

Keywords: $\text{MgTiO}_3:\text{Sm}^{3+}$; Nanophosphor; J-O Parameters; Photoluminescence; CIE N CCT;

1. Introduction

Inorganic luminescent materials doped with Sm^{3+} found its use in counterfeit light creation, white light-emitting diodes (LEDs) with high effectiveness and natural wellbeing [1-3]. Till today, commercial WLEDs have been based on the combination of LED with blue and yellow light. They have poor color render index (CRI), which can be solved by using tricolor (red, green and blue) phosphors energized by a near-ultraviolet (NUV) energy. This leads to the preparation of new efficient phosphors for new generation WLEDs [4-7]. In recent years, ABO_3 perovskite structures [8, 9] have turned out to be very vital materials as host segments in numerous applications [3]. Magnesium titanate (MgTiO_3), an excellent host material, can find a place in the perovskite group of mixes with ABO_3 structure and be a member of the ilmenite group ($E_g \sim 4$ eV) [10].

MgTiO_3 was prepared using different wet and soft blend techniques including polymerized complex strategy, sol-gel process, co-precipitation method, etc [11]. However, solution combustion synthesis (SCS) method has been developed and successfully used for the low temperature production of pure and doped nanoparticles in the past few years [5]. In the present study, Sm^{3+} doped MgTiO_3 phosphor is prepared by SCS.

2. Experimental

2.1. Synthesis of $\text{MgTiO}_3:\text{Sm}^{3+}$

$\text{MgTiO}_3:\text{Sm}^{3+}$ phosphors were prepared by solution combustion method [8] using urea as a fuel. Stoichiometric quantities of start-

ing materials were mixed well in a petridish with little amount of distilled water and was put in a muffle furnace (500 ± 10 °C). Thereafter, the reaction was initiated finally leaving a white powder.

2.2. Characterization

Shimadzu X-ray diffractometer (operating at 50 kV and 20 mA by means of $\text{CuK}\alpha$ (1.541 Å) radiation with a nickel filter) was used for PXRD. JEOL, JEM-2100 (accelerating voltage up to 200 kV, LaB_6 filament) for TEM analysis and Shimadzu UV-Vis spectrophotometer model 2600 for DRS. Photoluminescence studies were carried out using a Hitachi F-4600 fluorescence spectrometer at RT with Xe lamp as a light source.

3. Results and discussions

3.1. Photometric properties

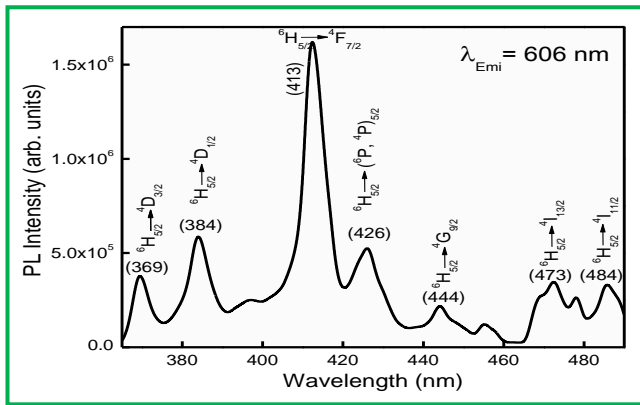


Fig. 1: Excitation Spectra of MgTiO₃:Sm³⁺ (5 mol %) nanophosphors.

Various transitions are possible among 4f energy levels of Sm³⁺ with 4f⁵ configuration. With this idea, we recorded the excitation spectrum of MgTiO₃:Sm³⁺ (5mol %), keeping the emission at ~607 nm (Fig. 1). Peaks between 350 to 500 nm were credited to f-f change of Sm³⁺ particles. Excitation peaks at ~369, ~384 and 413 nm connected to ⁶H_{5/2}→⁴D_{3/2}, ⁶H_{5/2}→⁶P_{7/2} + ⁴K_{13/2} and ⁶H_{5/2}→⁴F_{7/2} transitions respectively [12]. PLE spectra showed the peak at 413 nm compared to the change of ⁶H_{5/2}→⁴F_{7/2}, which gave more intense emission, due to resonance transfer of energy [13].

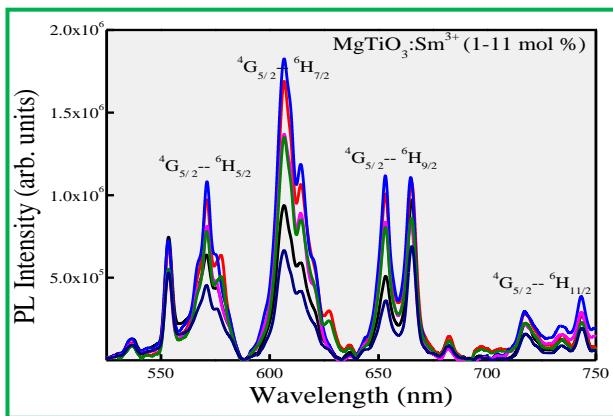


Fig. 2: Emission Spectra of MgTiO₃:Sm³⁺ (1-11 mol %) nanophosphors.

Fig. 2 shows that the emission spectra of Sm³⁺ ions doped MgTiO₃ (λ_{exc}-413 nm), the emission peaks were comparable to the change of ⁴G_{5/2}→⁶H_{5/2} (570 nm) magnetic-dipole (MD) transition, ⁴G_{5/2}→⁶H_{7/2} (607 nm) incompletely magnetic and somewhat constrained electric-dipole(ED), ⁴G_{5/2}→⁶H_{9/2} (658 nm) purely ED transition and ⁴G_{5/2}→⁶H_{11/2} (707 nm) the intra 4-f orbital transitions of Sm³⁺ [14-22] and show in the energy level graph (Fig. 3).

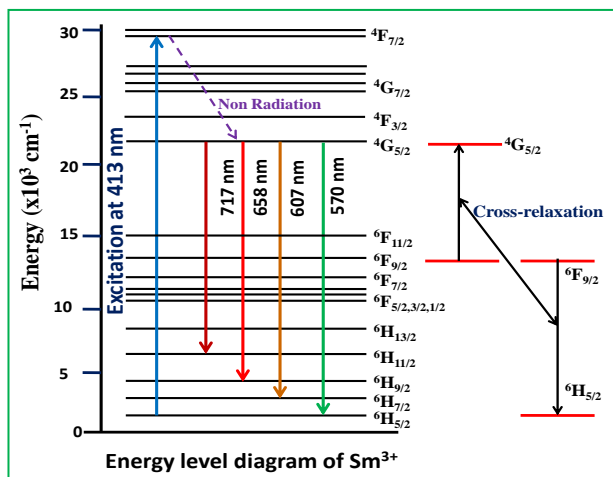


Fig. 3: Energy Level Diagram Indicating Emission Probabilities of Sm³⁺ in MgTiO₃ Host.

It was observed that at 5 mol percentage PL intensity was more and thereafter, concentration quenching happened [23] and non-radiative transitions increased because normal collaboration, separate between Sm ions diminished thereby diminishing the PL intensity (Fig 4). As Blasse [24] suggested, the critical energy transfer distance (R_c) was calculated to know non-radiative energy transfer process, which was found to be 3.2 Å (<5 Å) [22], showing that the exchange interaction was responsible between samarium ion in this host.

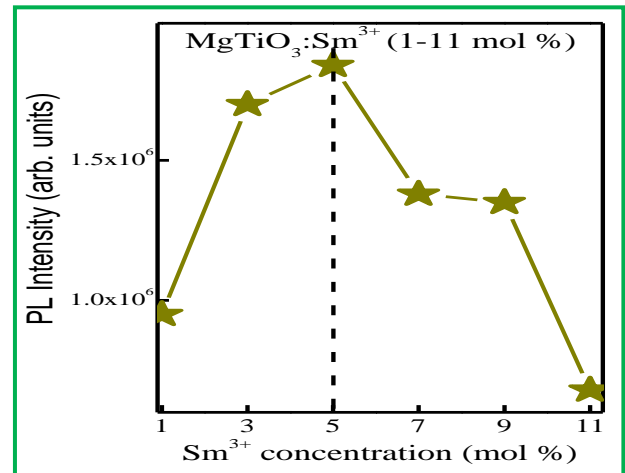
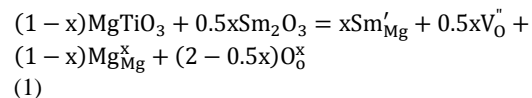


Fig. 4: Variation of PL Intensity with Respect to Sm³⁺ concentration.

The possible defect mechanism for non radiative energy transfer was proposed as,



where ‘Sm’_{Mg}’ means ‘Sm’ occupying the Mg²⁺ site, ‘V₀’ was the ‘O²⁻’ vacancy, ‘Mg_{Mg}^x’ represents the rest Mg atoms and ‘O₀^x’ (oxygen in MgTiO₃) [25]. Also, Dexter theory was used to find the value Q [26], $\left\{\frac{1}{x} = k [1 + \beta(x)^{\frac{2}{3}}]^{-1}\right\}$, Q = 6, 8 and 10 for (d-d), (d-q), (q-q) collaborations separately [27]. By assuming β(X)^{Q/3}>> 1, it show $\left\{\log\left(\frac{1}{x}\right) = k' - \frac{Q}{3} \log x\right\}$, using the plot of log 1/x v/s log x (Fig. 5), Q=3.09 (close to 3), indicates that exchange collaboration is in charge of concentration quenching.

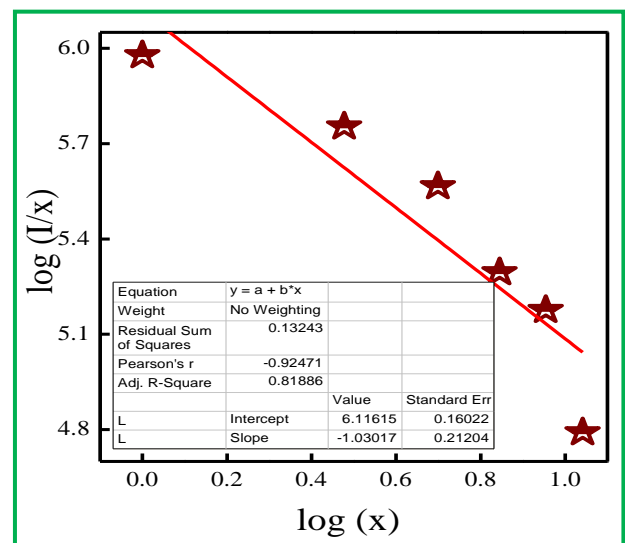


Fig. 5: Relation between Log(X) and Log (1/X) Sm³⁺ (1- 11 mol %) doped MgTiO₃.

The color coordination (CIE) and relevant color temperature (CCT) of the samples were calculated for MgTiO₃:Sm³⁺ (1-11 mol %) phosphors and is shown in Fig. 6. It was observed that orange red emission by the present phosphor and CCT (Fig. 7) [28], [29] was found to be 2036 K (<5000 K).

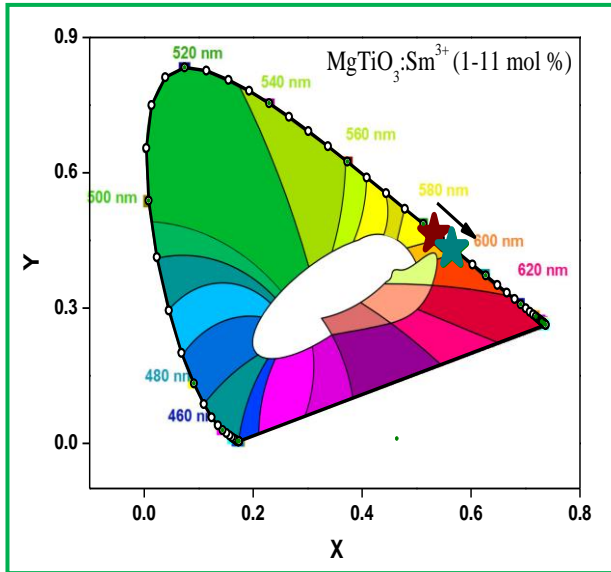


Fig. 6: CIE Diagram of MgTiO₃:Sm³⁺ (1-11 mol %) nanophosphor.

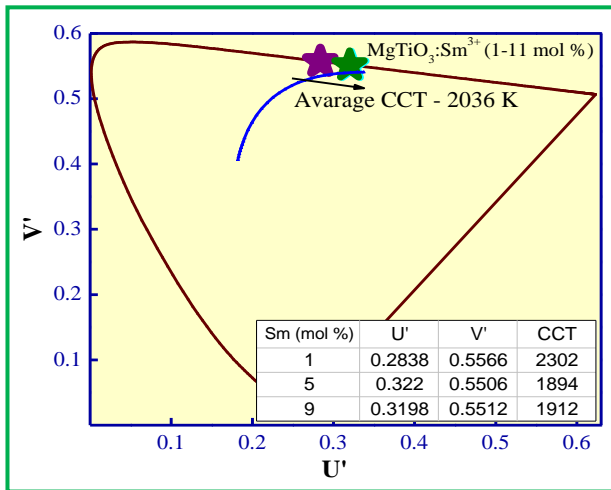


Fig. 7: CCT Diagram of MgTiO₃:Sm³⁺ (1-11 mol %) nanophosphor.

3.2. Judd-OFELT analysis of MgTiO₃:Sm³⁺ (1-11 mol %) nanophosphors

The Judd-Ofelt (J-O) hypothesis was utilized to contemplate the spectral performance, and all the J-O parameters ($\Omega \lambda$ ($\lambda = 2, 4$ and 6)) could be evaluated from the PL emanation data [30-32].

Table 1: Judd-Ofelt Parameters of MgTiO₃:Sm³⁺ Nanophosphors ($\lambda_{\text{exi}} = 413 \text{ nm}$)

Sm ³⁺ Mol %	J-O Intensity Parameters ($\times 10^{22} \text{ Cm}^2$)		Transitions	A _R (S ⁻¹)	A _{NR} (S ⁻¹)	A _T (S ⁻¹)	τ_{Rad} (Ms)	H (%)	B (%)
	Ω_2	Ω_4							
1	0.9660	0.6393	⁴ G _{5/2} → ⁶ H _{5/2}	93.11	27.79	120.9	10.73	77.01	56.27
3	1.0111	0.5389		94.75	20.85	115.6	10.55	81.96	56.22
5	0.9879	0.6170	⁴ G _{5/2} → ⁶ H _{7/2}	96.40	22.60	119.0	10.37	81.00	56.24
7	0.9896	0.6236		95.59	22.81	118.4	10.46	80.73	56.24
9	0.9947	0.6332	⁴ G _{5/2} → ⁶ H _{9/2}	95.18	23.02	118.2	10.50	80.50	56.23

The spontaneous emission probability of $4G_{5/2} \rightarrow 6H_{5/2}$ is given by [33].

$$A_{5/2-5/2} = \frac{64\pi^4 v_j^3 n^3 S_{\text{md}}}{3h(2J+1)} \quad (2)$$

The ED transition ($A_{5/2J}$) of $4G_{5/2} \rightarrow 6H_J$ ($J = 7/2$ and $9/2$) is given by

$$A_{5/2J} = \frac{64\pi^4 v_j^3}{3h(2J+1)} e^2 \frac{n(n^2+2)^2}{9} \sum_{\lambda=2,4,6} \Omega_{\lambda} |\langle ^4G_{5/2} \| U^{\lambda} \| ^6H_J \rangle|^2 S_{\text{md}} \quad (3)$$

The MD line strength and n ; refractive index is given by [34-35].

$$n = xn_b + (1-x)n_m \quad (4)$$

Where n_b ; refractive index of the bulk, x ; optical filling factor and x can be controlled by utilizing the connection

$$x = \frac{n_s - n_m}{n_b - n_m} \quad (5)$$

Where n_s the R.I of the sample. J-O parameters can be controlled by utilizing the connection

$$\frac{\int I_j dv}{\int I_{5/2} dv} = \frac{A_{5/2J}}{A_{5/2-5/2}} = \frac{e^2 v_j^3 (n^2+2)^2}{S_{\text{md}} v_{5/2}^3 9n^2} \Omega_{\lambda} |\langle ^4G_{5/2} \| U^{\lambda} \| ^6H_J \rangle|^2 \quad (6)$$

In all the nanophosphor the trend $\Omega_2 > \Omega_4$ was rather expected [36].

The add up to radiative progress (AR) was controlled by

$$A_R = \sum_J A_{5/2J} = A_{5/2-5/2} \frac{v_{5/2-5/2}}{I_{5/2-5/2}} \sum_{J=5/2}^{9/2} \frac{I_{5/2J}}{v_{5/2J}} \quad (7)$$

$A_{5/2-5/2}$: Einstein's coefficient. $I_{5/2J}$: integrated area of the emission spectrum.

The radiative lifetime (τ_{rad}) is determined by

$$\tau_{\text{rad}} = \frac{1}{\sum_J A_{5/2J}} = \frac{1}{A_R} \quad (8)$$

The luminescence quantum efficiency (η) was measured and found to be ~ 72 %.

$$\eta = \frac{A_R}{A_R + A_{NR}} = \frac{A_R}{A_T} \quad (9)$$

The branching ratio ($\beta_{5/2J}$) was expressed as [48]

$$\beta_{5/2J} = \frac{A_{5/2J}}{\sum A_{5/2J}} \quad (10)$$

All the J-O intensity parameters are tabulated in Table 1, showing that the present phosphor can be a potential candidate for warm WLED and solid state displays.

3.3. Crystallite size and band gap analysis

- [16] Zhang, R. Hu, Q. Qin, D. Wang, B. Liu, Y. Wen, M. Zhou, Y. Wang, J. Lumin. 132 (2012) 2590-2594. <https://doi.org/10.1016/j.jlumin.2012.05.027>.
- [17] Liurong Shi, Jiachi Zhang Huihui Li, PengfeiFeng, Xue Liu, Zhongqiu Fu, Yuhua Wang, J. Alloys compd. 579 (2013) 82–85 <https://doi.org/10.1016/j.jallcom.2013.05.056>.
- [18] Zhongfei Mu, Yihua Hu, Li Chen, Xiaojuan Wang, GuifangJu, Zhongfu Yang, YahongJin, J. Lumin. 146 (2014) 33–36 <https://doi.org/10.1016/j.jlumin.2013.09.043>.
- [19] Q. Zeng, H.B. Liang, Z.F. Tian, H.H. Lin, Q. Su, Chin. J. Inorg. Chem. 24 (2008) 333-342.
- [20] Ruijin Yu, HyeonMi Noh, ByungKee Moon, Byung Chun Choi, Jung Hyun Jeong, Ho Sueb Lee, Kiwan Jang, Soung Soo Yi, J.lumin 145(2014)717–722 <https://doi.org/10.1016/j.jlumin.2013.08.049>.
- [21] G.S.R. Raju, S. Buddhudu, Spectrochim. Acta, Part A 70 (2008) 601-605. <https://doi.org/10.1016/j.saa.2007.08.004>.
- [22] V. Singh, S. Watanabe, T.K.G. Rao, J.F.D. Chubaci, H.Y. Kwak, J. Non-cryst. Solids 356 (2010) 1185-1190. <https://doi.org/10.1016/j.jnoncrysol.2010.03.007>.
- [23] Z. Wang, P. Li, Z. Yang, Q. Guo, J. Lumin. 132 (2012) 1944–1948. <https://doi.org/10.1016/j.jlumin.2012.03.022>.
- [24] G. Blasse, Philips Res. Rep. 24 (1969) 131–144.
- [25] S. Shi, M. Hossu, R. Hall, W. Chen, J. Mater Chem. 22 (2012) 23461-23467. <https://doi.org/10.1039/c2jm34950g>.
- [26] S. Som, P. Mitra, Vijay Kumar, Vinod Kumar, J.J. Terblans, H.C. Swart, S.K. Sharma, Dalton Trans. 43 (2014) 9860–9871. <https://doi.org/10.1039/C4DT00349G>.
- [27] B. Devakumar, P. Halappa, C. Shivakumara, Dye Pigm. 137 (2017) 244-255. <https://doi.org/10.1016/j.dyepig.2016.10.016>.
- [28] Z. Mu, Y. Hu, L. Chen, X. Wang, G. Ju, Z. Yang, Y. Jin, J. Lumin. 46(2014) 33–36. <https://doi.org/10.1016/j.jlumin.2013.09.043>.
- [29] Som S, Das S, Dutta S, Visser HG, Pandey MK, Kumar P, Dubey RK and Sharma S K, RSC Adv. 5(2015) 70887–98.
- [30] J. Li, J.G. Li, S. Liu, X. Li, X. Sun, Y. Sakka, Sci. Technol. Adv. Mater. 14 (2013) 054201-054210. <https://doi.org/10.1088/1468-6996/14/5/054201>.
- [31] Q.L. Dai, H.W. Song, M.Y. Wang, X. Bai, B. Dong, R.F. Qin, X.S. Qu, H. Zhang, J. Phys. Chem. C 112 (2008) 19399–19404. <https://doi.org/10.1021/jp808343f>.
- [32] S.K. Gupta, N. Pathak, S.K. Thulasidas, V. Natarajan, J. Lumin. 69 (2016) 669–673. <https://doi.org/10.1016/j.jlumin.2014.10.009>.
- [33] Z. Mu, Y. Hu, L. Chen, X. Wang, G. Ju, Z. Yang, Y. Jin, J. Lumin. 46(2014) 33–36. <https://doi.org/10.1016/j.jlumin.2013.09.043>.
- [34] W.T. Carnall, P. R. Fields, K. Rajnak, J. chem. Phys 49 (1968) 4412-4423. <https://doi.org/10.1063/1.1669892>.
- [35] S. Som, Subrata Das, S. Dutta, Hendrik G. Visser, Mukesh Kumar Pandey, Pushpendra Kumar, Ritesh Kumar Dubey and S. K. Sharma, RSC Adv. 5 (2015) 70887–70898. <https://doi.org/10.1039/C5RA13247A>.
- [36] A. Agarwal, I. Pal, S. Sanghi, M.P. Aggarwal, Opt. Mater. 32 (2009) 339- 344. <https://doi.org/10.1016/j.optmat.2009.08.012>.
- [37] Zhang Jian, YIN Jing, LIU Panpan, GAO Bin, BIE Lijian, J. Rare Earth. 30 (2012) 1009. [https://doi.org/10.1016/S1002-0721\(12\)60170-7](https://doi.org/10.1016/S1002-0721(12)60170-7).
- [38] K.M. Girish, Ramachandra Naik, S.C. Prashantha, H. Nagabhushana, H.P. Nagaswarupa, K.S. AnanthaRaju, H.B. Premkumar, S.C. Sharma, B.M. Nagabhushana, Spectr Act Part A: Molec and BiomoSpectr, 138 (2015) 857–865. <https://doi.org/10.1016/j.saa.2014.10.097>.
- [39] C. Shivakumara, R. Saraf, P. Halappa, Dye Pigm. 126 (2016) 154–164. <https://doi.org/10.1016/j.dyepig.2015.10.032>.
- [40] J.B. Prasannakumar, G. Ramgopal, Y.S. Vidya, K.S. Anantharaju, B. Daruka Prasad, S.C. Sharma, S.C. Prashantha, H.B. Premkumar, H. Nagabhushana, Spectr Act Part A: Molec and BiomoSpectr, 141 (2015) 149-160.
- [41] R.C. Aguielera, Z. Han, Y. Cai, L.C. Kimerling, J. Michel, Appl. Phys. Lett. 102 (2013) 152106. <https://doi.org/10.1063/1.4802199>.
- [42]